Published in final edited form as:
Eur Polym J. 2011 February 1; 47(2): 162–170. doi:10.1016/j.eurpolymj.2010.11.007.

Characterization of dimethacrylate polymeric networks: a study of the crosslinked structure formed by monomers used in dental composites

Carmem S. Pfeifer[Research Assistant Professor],
University of Colorado, School of Dental Medicine, Craniofacial Biology, 12800 E 19th ave, Aurora, CO, USA, 80045. carmem.pfeifer@ucdenver.edu, Ph: 1-303-724-1046, Fax: 1-303-724-1945

Zachary R. Shelton[Undergraduate student],
University of Colorado, School of Dental Medicine, Craniofacial Biology, 12800 E 19th ave, Aurora, CO, USA, 80045. Zachary.shelton@ucdenver.edu

Roberto R. Braga[Professor],
University of São Paulo, School of Dentistry, Av. Prof. Lineu Prestes, 2227, São Paulo, SP, Brazil, 05508. rrbraga@usp.br

Dario Windmoller[Associate Professor],
Federal University of Minas Gerais, Chemistry Department, Av. Antônio Carlos, 6627, Belo Horizonte, MG, Brasil, 31270-901. dariow@ufmg.br

José C. Machado[Professor], and
Federal University of Minas Gerais, Chemistry Department, Av. Antôonio Carlos, 6627, Belo Horizonte, MG, Brasil, 31270-901. jcmachado@task.com.br

Jeffrey W. Stansbury[Professor]
University of Colorado, Chemical and Biological Engineering & School of Dental Medicine, Craniofacial Biology, 12800 E 19th ave, Aurora, CO, USA, 80045. jeffrey.stansbury@ucdenver.edu

Abstract

The resin phase of dental composites is mainly composed of combinations of dimethacrylate comonomers, with final polymeric network structure defined by monomer type/reactivity and degree of conversion. This fundamental study evaluates how increasing concentrations of the flexible triethylene glycol dimethacrylate (TEGDMA) influences void formation in bisphenol A diglycidyl dimethacrylate (BisGMA) co-polymerizations and correlates this aspect of network structure with reaction kinetic parameters and macroscopic volumetric shrinkage. Photopolymerization kinetics was followed in real-time by a near-infrared (NIR) spectroscopic technique, viscosity was assessed with a viscometer, volumetric shrinkage was followed with a linometer, free volume formation was determined by positron annihilation lifetime spectroscopy (PALS) and the sol-gel composition was determined by extraction with dichloromethane followed

Correspondence to: Carmem S. Pfeifer; Jeffrey W. Stansbury.

by ^{1}H-NMR analysis. Results show that, as expected, volumetric shrinkage increases with TEGDMA concentration and monomer conversion. Extraction/^{1}H-NMR studies show increasing participation of the more flexible TEGDMA towards the limiting stages of conversion/crosslinking development. As the conversion progresses, either based on longer irradiation times or greater TEGDMA concentrations, the network becomes more dense, which is evidenced by the decrease in free volume and weight loss after extraction in these situations. For the same composition (BisGMA/TEGDMA 60–40 mol%) light-cured for increasing periods of time (from 10 to 600 s), free volume decreased and volumetric shrinkage increased, in a linear relationship with conversion. However, the correlation between free volume and macroscopic volumetric shrinkage was shown to be rather complex for variable compositions exposed for the same time (600 s). The addition of TEGDMA decreases free-volume up to 40 mol% (due to increased conversion), but above that concentration, in spite of the increase in conversion/crosslinking, free volume pore size increases due to the high concentration of the more flexible monomer. In those cases, the increase in volumetric shrinkage was due to higher functional group concentration, in spite of the greater free volume. Therefore, through the application of the PALS model, this study elucidates the network formation in dimethacrylates commonly used in dental materials.

Keywords

Dental resins; free volume; polymer network; volumetric shrinkage; reaction kinetics

INTRODUCTION

Polymerizations of dimethacrylates form a complex crosslinked organic matrix, which is reinforced by the inclusion of inorganic fillers for some applications, such as dental composite restoratives. In composite materials, the filler can greatly influence properties like fracture toughness, hardness, elastic modulus, flexural strength and volumetric shrinkage [1]. However, depending on its composition and structure as well as its crosslink density and degree of heterogeneity, the organic matrix clearly plays an important role in property development [2,3]. Reaction kinetics parameters, final degree of conversion and the resistance to degradation in organic solvents are also dependent upon the molecular structure of the monomers employed [4,5]. When considered in conjunction, all these parameters help define the material's durability in the oral environment.

The most commonly used monomers in dental composites are bisphenol A diglycidyl dimethacrylate (BisGMA), its ethoxylated analog (BisEMA) and urethane dimethacrylates (UDMA) along with low molecular weight diluents, usually ethylene glycol derivatives, such as triethylene glycol dimethacrylate (TEGDMA). BisGMA presents a rigid crosslink structure with rotationally hindered aromatic rings and hydroxyl groups that form strong hydrogen bonds, which impair mobility and prevent the homopolymer from achieving high degrees of conversion [6]. When BisGMA is combined with more flexible comonomers, an increase in reactivity is typically observed along with polymerizations that progress to a higher degree of conversion [7]. TEGDMA has a very flexible aliphatic structure in which the ether linkages serve as hydrogen bond acceptors [8]. As the concentration of TEGDMA increases, a greater tendency to form microgels is observed due to the greater likelihood of primary and secondary cyclization [9,10], which may jeopardize polymer packing density and lead to a looser network structure [11]. This can be quantified by the fractional free volume of the material, *i.e.*, the unoccupied space between chains and side groups that is essential to allow molecular and cooperative motion within both linear and crosslinked polymers. Therefore, free volume is related to the concentration and size of pores among polymer chains [12]. Monomers with more limited cyclization potential, such as BisGMA, are also more likely to achieve gelation at an earlier stage in conversion [13,14]. Because of

the limited intramolecular hydrogen bonding, BisGMA forms more extended intermolecular interactions that lead to a relatively high monomeric glass transition temperature (−6 °C). Thus, in reactions near room temperature, the onset of vitrification occurs at fairly low degrees of conversion [15]. Both the degree of conversion and crosslink density increase in BisGMA systems combined with TEGDMA in increasing concentrations, but that is followed by a gradual decrease in flexural strength and an increase in volumetric shrinkage [16]. In this case, the increased volumetric shrinkage is due to both a higher reactive group concentration and the higher degree of conversion. TEGDMA likely provides shorter crosslinks on average compared with BisGMA, in spite of the similar separation between methacrylate groups in the extended chain conformations of both molecules [17]. It also has been demonstrated through analysis of leachable components at various stages of polymerization that the contribution of TEGDMA to network formation proportionally increases with conversion in copolymerizations with BisGMA, pointing to a compositional drift [18].

Many studies utilize the indirect method of polymer softening after immersion in organic solvents to estimate crosslinking density and evaluate tri-dimensional network formation. While this is a practical method, it provides only limited information, since it relies on other factors, such as the solubility parameters of the material and solvent. Positron Annihilation Lifetime Spectroscopy (PALS) allied with analysis of the gel fraction composition was used here as a means to evaluate network structure on the sub-nanometer scale. Increasing concentrations of TEGDMA monomer in BisGMA solutions were employed with the intent that comonomer composition affects degree of conversion and reaction kinetics. Different rates of polymerization, in turn, previously have been shown to affect free volume entrapment within the network [19,20], but a correlation with overall, macroscopic volumetric shrinkage and composition of extracted components has not been established. To gain insight into how the complex interaction between molecular structure and overall conversion impacts network formation, the present study tests the hypothesis that free volume decreases as a function of 1) the increase in conversion provided by increasing TEGDMA concentrations and 2) the increase in TEGDMA's contribution to network formation at higher conversions.

MATERIALS AND METHODS

Specimen preparation and experimental design

Chemicals were used as received; all monomers were donated by ESSTECH (Essington, PA, USA).Bisphenol A diglycidyl dimethacrylate (BisGMA) was mixed with a secondary monomer (triethylene glycol dimethacrylate - TEGDMA) in concentrations ranging from 0 to 100 mol%, in 20 % increments. For each, 0.6 wt% of a tertiary amine (ethyl N,N-dimethylaminobenzoate - EDMAB) and 0.2 wt% of a photosensitizer (dl-camphoroquinone - CQ) were added; all were obtained from Sigma Aldrich (St. Louis, MO, USA).

Kinetics of conversion by near-IR and mid-IR analysis of hydrogen bonding formation

Monomeric materials were placed in a silicon rubber mold (10 mm in diameter × 1.2 mm in thickness) sandwiched between two glass slides, then clamped in a holder inside the IR chamber (Nicolet Nexus 6700, Thermo Scientific, Waltham, MA, USA). The peak area correspondent to the vinyl stretching absorption in the near-IR spectrum (6165 cm^{-1}) [21] was followed during continuous irradiation (320–500 nm light, at 100 mW/cm^2, Acticure 4000, EXFO, Ontario, Canada) for 10 min. The composition BisGMA/TEGDMA 60/40 mol % was also photoactivated for 10, 20, 30 or 60 s while the kinetic profile was recorded for 10 min. The specimens were stored dry at room temperature for 24 h prior to being used in the free volume and extraction experiments described in the following sections.

One drop of the unpolymerized materials was sandwiched between NaCI plates for mid-IR analysis of hydrogen bonding interactions based on the characteristic OH absorption band observed at approximately 3500 cm^{-1} [22]. The OH absorbance increases in area and the peak maxima shifts to longer wavelengths with increasing hydrogen bond strength [6,22].

Volumetric shrinkage

Volumetric shrinkage was assessed with a linometer (ACTA Foundation, Netherlands). A drop of monomer was sandwiched between a glass slide and an aluminum disc, which in turn is positioned above a non-contact probe. The light guide (100 mW/cm^2, 320–500 nm, Acticure 4000, EXFO, Ontario, Canada) was placed on top of the glass slide. As the material polymerizes and shrinks, the aluminum disc is lifted and the difference in potential sensed by the probe is recorded by the software. The dynamic linear shrinkage results were followed for the duration of the light exposure (10 min) and later converted to volumetric shrinkage data as described previously [23].

Free volume experiments

Free volume was determined by positron annihilation lifetime spectroscopy (PALS). In this technique, the antimatter of the electron (positron) is injected into a solid and, upon encountering an electron, it is either immediately annihilated or forms a meta-stable positronium complex with very limited lifetimes that depend on whether the spins are parallel or anti-parallel (o-Ps or p-Ps, respectively). Gamma photons are released in the process, and that is what is recorded by the detector. If positrons end up in a region of the material that is scarce in electrons (such as a void), their lifetime will be extended compared to those in an electron-dense region. By comparing positron lifetimes and signal intensities in different materials, the size and distribution of nanopores (or free volume among polymer chains) can be calculated.

The PALS experiments were carried out in air atmosphere at 294±1 K in an ORTEC fast-fast coincidence system with temporal resolution of 290 ps. NaCI (Amersham) with ~15 μCi activity prepared between two 7 μm thick Kapton foils was used as the positron source, which was sandwiched with the samples in the form of pellets 1.2 mm thick with approximate area of 8 × 8 mm^2. The three-component analysis of a minimum of three lifetime spectra with ~10^6 total coincidence counts obtained at 294 K and by Positronfit Extended Program yielded lifetime ($\delta 1$) and relative intensity (I_i) parameters, where i = 1,2,3 represents the species p-Ps, e+ (free positron annihilation), and o-Ps, respectively.

For the obtained lifetimes, the shortest component (δ=0.125 ns) associated with p-Ps, was fixed during the spectral analysis. The no-constraint analysis furnished similar results considering the experimental error. The lifetimes obtained in the spectral analysis are average values of the positronic species lifetime distributions. The free volume size also represents an average value.

Extraction studies: Leachable components and compositional drift during polymerization

After being submitted to the kinetics protocol, specimens were weighed and conversion was determined prior to the immersion in 8 mL of methylene chloride containing 0.01 wt% BHT (2,6-di-tert-butyl-4-methylphenol, Sigma Aldrich) for 48 h. The use of BHT is intended to avoid further conversion due to the increased molecular mobility produced in solvent-swollen networks. After the first storage period, the solvent was collected and the specimens were placed in 8 mL of pure methylene chloride for at least 4 weeks. The solvent from the extraction solutions was removed under rotary evaporation to constant mass and ^{1}H-NMR spectra were obtained from the extracts to determine the composition on the sol fraction. The remaining discs were dried to a constant mass and weighed after extraction as well.

Viscosity

Viscosity measurements of the monomer mixtures were assessed in a viscometer (CAP 200 + Viscometer, Brookfield Engineering Laboratories, MA; USA) at room temperature (23 °C) using a 14 mm diameter spindle at 200 rpm (hold time: 15 s; run time: 30 s).

Statistical analysis

Data was analyzed with one-way ANOVA and Tukey's test for contrast between averages, at a global significance level of 95%.

RESULTS and DISCUSSION

Even though it was not the objective of this paper to describe the kinetic behavior of dimethacrylates, which has been extensively explored in the literature [8,24–27], some key aspects (summarized in Table 1) will be highlighted to better explain network formation. As expected and previously demonstrated, [2,3,28] when BisGMA and TEGDMA are co-polymerized, both the conversion and the maximum rate of polymerization increase compared to the neat monomers (Table 1). One of the reasons is the logarithmic decrease in viscosity given by the systematic addition of TEGDMA to the bulky, hindered BisGMA molecule (Table 1). The viscosity has a more pronounced effect on segmental movements of radicals at the early stages of polymerization, affecting the rate of polymerization before the medium mobility becomes restricted due to network formation [15]. Indeed, the rate at 10 % conversion observed for the BisGMA/TEGDMA 60–40 mol% composition was the highest, as it has been demonstrated that in this concentration the initial viscosity is optimized to delay autoacceleration to slightly higher conversion [17], when it coincides with the development of high radical concentrations, which is not the case at the onset of most polymerizations. This fits with the fact that conversion at R_p^{max} is not the lowest for the optimized formulation. At TEGDMA concentrations higher than that, both the lower initial viscosity and the greater tendency towards cyclization during polymerization combine to extend the amount of network formation necessary to reach the mobility limitation threshold that allows effective autoacceleration. Cyclization contributes to conversion, but not to overall network development, and leads to heterogeneity [29,30]. Cyclic structures provide enhanced overall mobility, as well as increase the mobility of pendant groups and crosslinks, with an effect analogous of that of plasticizers [29]. This means vitrification is reached at higher conversion.

The evaluation of the free volume is being proposed here not only as an alternative technique to assess network structure, in place of indirect methods based on polymer softening after immersion in organic solvents, but also to allow for correlations between pore formation and the macroscopic manifestation of shrinkage. Positron annihilation lifetime spectroscopy technique (PALS) utilizes gamma radiation to annihilate the anti-electron (positron), yielding a positronium atom of known radius (1.06 Å), used as sub-nanometer probe to study the microstructure of polymer systems, in relation to the free volume holes present between chains [31]. The free volume increased with TEGDMA concentration, and this increase was more pronounced above 60 % TEGDMA. The homopolymer of TEGDMA presents 20 % higher free volume compared to pure BisGMA, which is an indication of poorer polymer packing. As opposed to BisGMA structure which engages in π-π stacking interactions between aromatic rings in addition to strong hydrogen bonding interactions, TEGDMA pendant groups and crosslinks are more flexible and more prone to rotational motion and tend to occupy more space (Scheme 1). This was true in spite of the 30 % higher conversion achieved by neat TEGDMA. This provides a demonstration that compared to simple density measurements, free volume characterization offers a more critical comparison of materials of differing copolymer compositions. The higher conversion

and lower molecular weight of TEGDMA explain the increased volumetric shrinkage afforded by TEGDMA rich formulations (Table 2). As a consequence of the faster rates of reaction observed for the co-monomer systems with higher TEGDMA content, greater excess free volumes were also expected due to the comparatively much slower rate of chain relaxation [19], which results in more heterogeneous structures at limiting conversion [32]. This is further complicated by the tendency to cyclization presented by TEGDMA. In turn, BisGMA contributes stronger hydrogen bonding interactions, as demonstrated by mid-IR analysis of the O-H interactions around 3500 cm^{-1} that show not only an increase in the peak area (normalized for concentration using the aromatic peak area) but also a shift in the peak maxima to longer wavelengths (Figure 1) [6,22]. This, along with π-π stacking given by the rotationally hindered aromatic rings, accounted for better packing, which is also demonstrated in Figure 2, where the macroscopic volumetric shrinkage of all different compositions was normalized by conversion and plotted against BisGMA concentration. The validity of this normalization approach is reflected in the consistency displayed in the normalized shrinkage obtained for the 60:40 BisGMA/TEGDMA composition at increasing exposure times and conversion (Table 3). The concept of a characteristic methacrylate molar shrinkage coefficient has already been demonstrated [33,34]. In this manner, the theoretical shrinkage can be calculated as the product of initial double-bond concentration, degree of conversion and molar shrinkage coefficient. The conversion-normalized compositionally varied shrinkage values reported in Figure 2 highlight the role of the monomer molecular weight in shrinkage development.

Comparisons between different compositions are potentially complicated by the fact that different levels of conversion are achieved at different rates, with both factors contributing to free volume (or polymer packing) determination in the final structure. Thus, a second series of experiments was carried out in which the same composition (BisGMA/TEGDMA at 60/40 mol %) was irradiated with increasing light exposure durations, at a fixed irradiance. As expected, the conversion increased with exposure time (Table 3), while the maximum rates of polymerization remained constant. The free volume showed a strong, negative relationship with conversion (r^2=0.996, Figure 3a), demonstrating that molecule packing, within the same composition, increases with polymerization. This highlights the poorer packing achieved with greater concentrations of more flexible TEGDMA, as opposed to the planar structure of BisGMA, in spite of the higher conversion, as denoted by the higher free volume obtained in the TEGDMA-rich groups. A greater reduction in free volume is observed in the lower conversion regime; conversely, a diminished free volume reduction is associated with high conversion (Figure 3a). A possible explanation is that at low conversion, free volume is more dependent on attachment of highly mobile free monomer, while at high conversion, nanopore size and distribution relies on a greater contribution from less mobile pendant group attachment to form crosslinks.

When the macroscopic volumetric shrinkage is considered, strong direct correlations with conversion were shown both for different compositions and for different exposure times (Figure 4), as previously demonstrated [35,36]. For the same composition exposed for different periods, the correlation between volumetric shrinkage and conversion was linear, whereas for the series of different compositions, that correlation followed a second order polynomial (Figure 4), as explained by the greater initial double bond concentration provided by TEGDMA. It develops that the correlation between free volume and volumetric shrinkage is somewhat weak for the different compositions (Figure 5) or, in other words, the macroscopic volumetric manifestation of conversion does not necessarily reflect nanopore formation within the network. Allied to higher conversion, another explanation for the augmented pore fraction to have been accompanied by slightly greater shrinkage is the higher rate of polymerization presented by the TEGDMA-rich formulations, which could potentially increase both cyclization and heterogeneity. One previous study on

dimethacrylates has already demonstrated that higher rates of polymerization achieved with higher irradiance lead to greater free volume formation in glassy polymers, especially at conversion levels above 10%, when chain relaxation is impaired by network formation, as previously mentioned [37]. In other words, because polymerization starts randomly in the bulk of the material, higher rates lead to the rapid formation of a stiff framework with a larger number of pores entrapped in it. In regards to the same composition at different conversions, a trend can be identified of increased volumetric shrinkage with decreasing free volume (Figure 5), probably because in that case, not only were the rates of polymerization similar, but also because the contribution to crosslinking from free monomer versus pendant functional groups at lower and higher conversion levels, respectively, may have influenced nanopore formation, as previously mentioned.

The extraction study was designed to identify a likely compositional drift with conversion [25], but also to possibly establish a correlation between the TEGDMA participation in network formation and free volume before and after extraction of leachable components. Methylene chloride was selected as the solvent to avoid the disparity in solubility of BisGMA and TEGDMA in water, the most commonly used immersion media, since it has been previously pointed out that the leached amount of the more hydrophobic BisGMA is dramatically underestimated with the use of aqueous extraction solutions [4,18]. The weight loss after extraction increased with BisGMA concentration in the starting mixture, more so above 60 mol % BisGMA (Figure 6), and that was most likely due to the decrease in conversion already discussed (Table 1). When weight loss is plotted against exposure time (for BisGMA/TEGDMA 60/40), again the effect of decreased conversion can be observed (Figure 6). ^{1}H-NMR spectra taken from the extract does not show evidence of broadening of the vinyl resonance peak nor does it show signal in the saturated aliphatic region (<1.5 ppm) [22], which would be indicative of the presence of oligomers. Increasing BisGMA content in the starting composition leads to an increase in the absolute weight loss, due to a reduction in conversion (Figure 7-C). The contribution of BisGMA to leached components (as determined by ^{1}H-NMR) in regards to the initial composition increases with conversion (Table 3,Figure 7-B and 7-D), pointing to an increasing participation of TEGDMA in network formation towards the limiting conversion values, which corroborates previously demonstrated data [18]. It is interesting to note that the slight reduction in free volume after extraction (expected based on the collapse of the network after solvent is removed from the specimen) is greater for the lower conversion specimens (Table 3), explained by the larger amount of leached unreacted monomer.

When the same analysis is applied to the increasing TEGDMA composition series, where all the groups were photo-activated for 600 s, it is observed that after the extraction, the BisGMA contribution to the gel fraction was slightly lower than expected based on the starting composition. Even though the gel composition was not significantly different before and after extraction, the reduction in BisGMA concentration in the gel tended to be more accentuated towards the higher BisGMA concentrations (Table 2), which can be explained by their lower conversion, as discussed previously. The fact that the free volume after extraction followed the same trends observed prior to extraction (TEGDMA richer mixtures presented overall higher free volume) agrees with the BisGMA contribution to the gel fraction data, with a less pronounced decrease in free volume compared to what was observed for the conversion series experiments.

This study has demonstrated that higher TEGDMA contents in the gel portion, as well as higher limiting conversion, result in lower free volume loss after extraction (even though in the case of TEGDMA-rich mixtures the overall free volume might be higher because of the greater freedom to rotation associated with these molecules), pointing to the expected increase in crosslinking density. Through the application of PALS to model monomers

widely used in dental materials, this study has demonstrated the correlation between molecular flexibility and resulting free volume, which shows this to be a reliable technique to predict the heterogeneity of a polymer network.

Acknowledgments

The authors thank ESSTECH for the donation of monomers used in this study and Septodont/Confidental for the use of the linometer. Matthew Barros is also acknowledged for the help with ^{1}H-NMR data collection. Support: NIH/NIDCR - 2R01DE14227.

References

1. Condon JR, Ferracane JL. Assessing the effect of composite formulation on polymerization stress. Jnl Amer Dent Assoc. 2000; 131(4):497–503.
2. Asmussen E, Peutzfeldt A. Influence of UEDMA BisGMA and TEGDMA on selected mechanical properties of experimental resin composites. Dent Mater. 1998; 14(1):51–56. [PubMed: 9972151]
3. Asmussen E, Peutzfeldt A. Influence of pulse-delay curing on softening of polymer structures. Jnl Dent Res. 2001; 80(6):1570–1573.
4. Ferracane J, Marker V. Solvent degradation and reduced fracture toughness in aged composites. Jnl Dent Res. 1992; 71(1):13–19.
5. Lovell LG, Stansbury JW, Syrpes DC, Bowman CN. Effects of composition and reactivity on reaction kinetics of dimethacrylate/ dimethacrylate copolymerizations. Macromolecules. 1999; 32(12):3913–3921.
6. Lemon MT, Jones MS, Stansbury JW. Hydrogen bonding interactions in methacrylate monomers and polymers. J Biomed Mater Res A. 2007; 83(3):734–746. [PubMed: 17559132]
7. Ogliari FA, Ely C, Zanchi CH, Fortes CB, Samuel SM, Demarco FF, Petzhold CL, Piva E. Influence of chain extender length of aromatic dimethacrylates on polymer network development. Dent Mater. 2007
8. Sideridou I, Tserki V, Papanastasiou G. Effect of chemical structure on degree of conversion in light-cured dimethacrylate-based dental resins. Biomaterials. 2002; 23(8):1819–1829. [PubMed: 11950052]
9. Young J, Kannurpatti A, Bowman C. Effect of comonomer concentration and functionality on photopolymerization rates, mechanical properties and heterogeneity of the polymer. Macrom Chem Phys. 1998; 199(6):1043–1049.
10. Sideridou I, Tserki V, Papanastasiou G. Study of water sorption, solubility and modulus of elasticity of light-cured dimethacrylate-based dental resins. Biomaterials. 2003; 24(4):655–665. [PubMed: 12437960]
11. Lopez-Suevos F, Dickens SH. Degree of cure and fracture properties of experimental acid-resin modified composites under wet and dry conditions. Dent Mater. 2008; 24(6):778–785. [PubMed: 17980422]
12. Machado JC, Silva GG, Oliveira FC, Lavall RL, Rieumont J, Licinio P, Windmoller D. Free-volume and crystallinity in low molecular weight poly(ethylene oxide). Jnl Pol Scie Part B - Pol Phys. 2007; 45:2400–2409.
13. Kloosterboer, JG.; Lijten, GFCM. Chain Cross-Linking Photopolymerization of Tetraethyleneglycol Diacrylate - Thermal and Mechanical Analysis. Acs Symposium Series; 1988. p. 409-426.
14. Anseth KS, Bowman CN. Kinetic Gelation Model Predictions of Cross-Linked Polymer Network Microstructure. Chem Eng Scie. 1994; 49(14):2207–2217.
15. Odian, G. Principles of polymerization. New York: Wiley-Interscience; 2004.
16. Floyd CJ, Dickens SH. Network structure of Bis-GMA- and UDMA-based resin systems. Dent Mater. 2006; 22(12):1143–1149. [PubMed: 16376422]
17. Dickens SH, Stansbury JW, Choi KM, Floyd CJ. Photopolymerization kinetics of methacrylate dental resins. Macromolecules. 2003; 36(16):6043–6053.

18. Stansbury JW, Dickens SH. Network formation and compositional drift during photo-initiated co-polymerization of dimethacrylate monomers. Polymer. 2001; 42(15):6363–6369.
19. Anseth KS, Kline LM, Walker TA, Anderson KJ, Bowman CN. Reaction-Kinetics and Volume Relaxation during Polymerizations of Multiethylene Glycol Dimethacrylates. Macromolecules. 1995; 28(7):2491–2499.
20. Anseth KS, Rothenberg MD, Bowman CN. A Photochromic Technique to Study Polymer Network Volume Distributions and Microstructure during Photopolymerizations. Macromolecules. 1994; 27(10):2890–2892.
21. Stansbury JW, Dickens SH. Determination of double bond conversion in dental resins by near infrared spectroscopy. Dent Mater. 2001; 17(1):71–79. [PubMed: 11124416]
22. Silverstein, R.; Webster, F.; Kiemle, D. Spectrometric identification of organic compounds. Hoboken, NJ: John Wiley & sons; 2005.
23. DeGee AF, Feilzer AJ, Davidson CL. True linear polymerization shrinkage of unfilled resins and composites determined with a linometer. Dent Mater. 1993; 9(1):11–14. [PubMed: 8299861]
24. Lovell LG, Stansbury JW, Syrpes DC, Bowman CN. Effects of composition and reactivity on the reaction kinetics of dimethacrylate/dimethacrylate copolymerizations. Macromolecules. 1999; 32(12):3913–3921.
25. Stansbury JW, Dickens SH. Network formation and compositional drift during photo-initiated copolymerization of dimethacrylate monomers. Polymer. 2001; 42(15):6363–6369.
26. Dickens S, Stansbury J, Choi K, Floyd C. Photopoymerization kinetics of methacrylate dental resins. Macromolecules. 2003; 36(16):6043–6053.
27. Cook WD, Forsythe JS, Irawati N, Scott TF, Xia WZ. Cure kinetics and thermomechanical properties of thermally stable photopolymerized dimethacrylates. J Appl Pol Scie. 2003; 90:3753–3766.
28. Cook W. Photopolymerization kinetics of dimethacryilates using the camphoroquinone/ amine initiator system. Polymer. 1992; 33(3):600–609.
29. Lovell LG, Newman SM, Bowman CN. The effects of light intensity, temperature, and comonomer composition on the polymerization behavior of dimethacrylate dental resins. Jnl Dent Res. 1999; 78(8):1469–1476.
30. Poshusta AK, Bowman CN, Anseth KS. Application of a kinetic gelation simulation to the characterization of in situ cross-linking biomaterials. Jnl Biomat Scie-Polymer Edition. 2002; 13(7):797–815.
31. Sousa A, Souza KC, Reis SC, Sousa RG, Windmoller D, Machado JC, Sousa EMB. Positron annihilation study of pore size in ordered SBA-15. Jnl Non-Crystall Solids. 2008; 354(42–44): 4800–4805.
32. Bowman CN, Peppas NA. Coupling of kinetics and volume relaxation during polymerizations of multiacrylates and multimethacrylates. Macromolecules. 1991; 24:1914–1920.
33. Patel MP, Braden M, Davy KWM. Polymerization Shrinkage of Methacrylate Esters. Biomaterials. 1987; 8(1):53–56. [PubMed: 3828447]
34. Dewaele M, Truffier-Boutry D, Devaux J, Leloup G. Volume contraction in photocured dental resins: the shrinkage-conversion relationship revisited. Dent Mater. 2006; 22(4):359–365. [PubMed: 16143380]
35. Braga RR, Ferracane JL. Contraction stress related to degree of conversion and reaction kinetics. Jnl Dent Res. 2002; 81(2):114–118.
36. Venhoven BA, de Gee AJ, Davidson CL. Light initiation of dental resins: dynamics of the polymerization. Biomaterials. 1996; 17(24):2313–2318. [PubMed: 8982470]
37. Anseth KS, Bowman CN, Peppas NA. Polymerization Kinetics and Volume Relaxation Behavior of Photopolymerized Multifunctional Monomers Producing Highly Cross-Linked Networks. Jnl Pol Scie Part A-Pol Chem. 1994; 32(1):139–147.

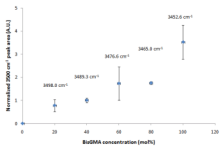

Figure 1.

Hydrogen bonding interactions of BisGMA/TEGDMA comonomer mixtures. The area under the peak at 3500 cm^{-1} was normalized for the methacrylate concentration in the mixture (by being divided by the aromatic peak area) and is shown in arbitrary units. Each data point is accompanied by the 3500 cm^{-1} peak position in wavenumbers.

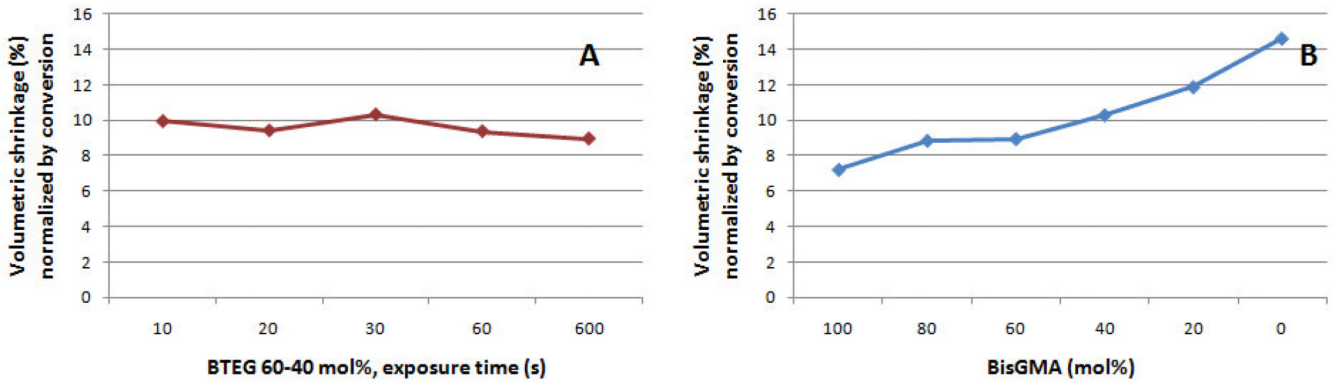

Figure 2.
Volumetric shrinkage normalized by conversion for a) BTEG 60–40 mol% exposed for increasing periods of time and b) for BisGMA combined to TEGDMA at different concentrations.

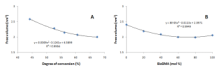

Figure 3.
Free volume as a function of (A) degree of conversion (%, obtained for 60:40 BisGMA/TEGDMA exposed for 10, 20, 30, 60 or 600 s) and (B) BisGMA concentration (mol% in varied BisGMA/TEGDMA compositions, all exposed for 600 s).

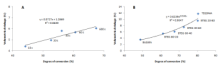

Figure 4.
Volumetric shrinkage as a function of degree of conversion for (A) degree of conversion (%, obtained for 60:40 BisGMA/TEGDMA exposed for 10, 20, 30, 60 or 600 s) and (B) BisGMA concentration (mol% in varied BisGMA/TEGDMA compositions, all exposed for 600 s).

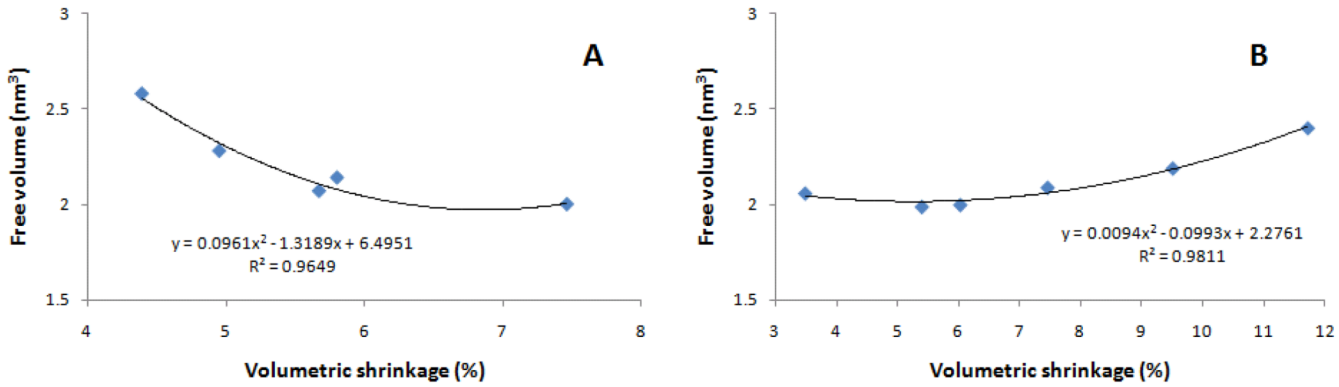

Figure 5.

Free volume as a function of volumetric shrinkage for (A) degree of conversion (%, obtained for 60:40 BisGMA/TEGDMA exposed for 10, 20, 30, 60 or 600 s) and (B) BisGMA concentration (mol % in varied BisGMA/TEGDMA compositions, all exposed for 600 s).

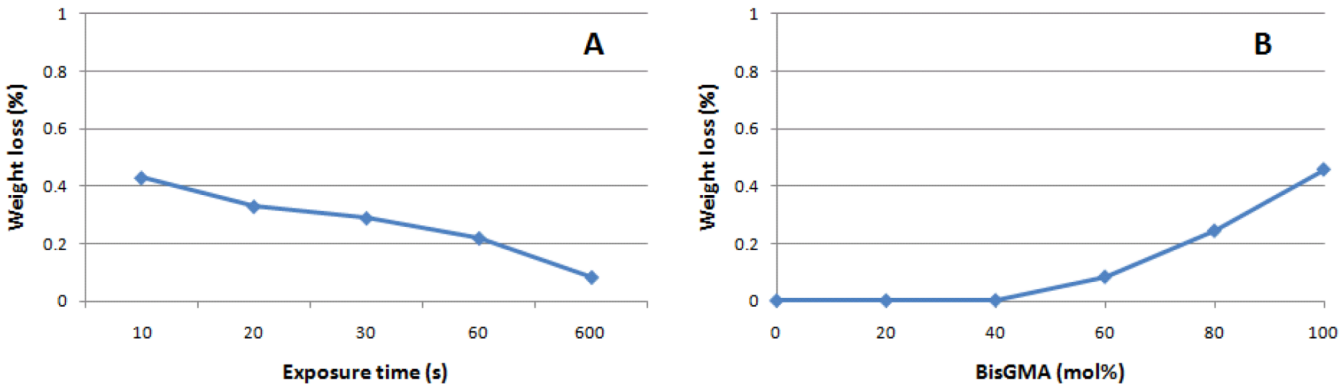

Figure 6.
Percentage weight loss after immersion in methylene chloride as a function of (A) degree of conversion (%, obtained for 60:40 BisGMA/TEGDMA exposed for 10, 20, 30, 60 or 600 s) and (B) BisGMA concentration (mol % in varied BisGMA/TEGDMA compositions, all exposed for 600 s).

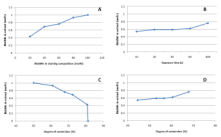

Figure 7.
NMR determination of BisGMA concentration in the extract as a function of (A) BisGMA concentration in the starting mixture, (B) exposure time, (C) degree of conversion (for all compositions exposed for 600 s) and (D) degree of conversion (for BisGMA/TEGDMA 60/40 exposed for 10, 20, 30, 60 or 600 s).

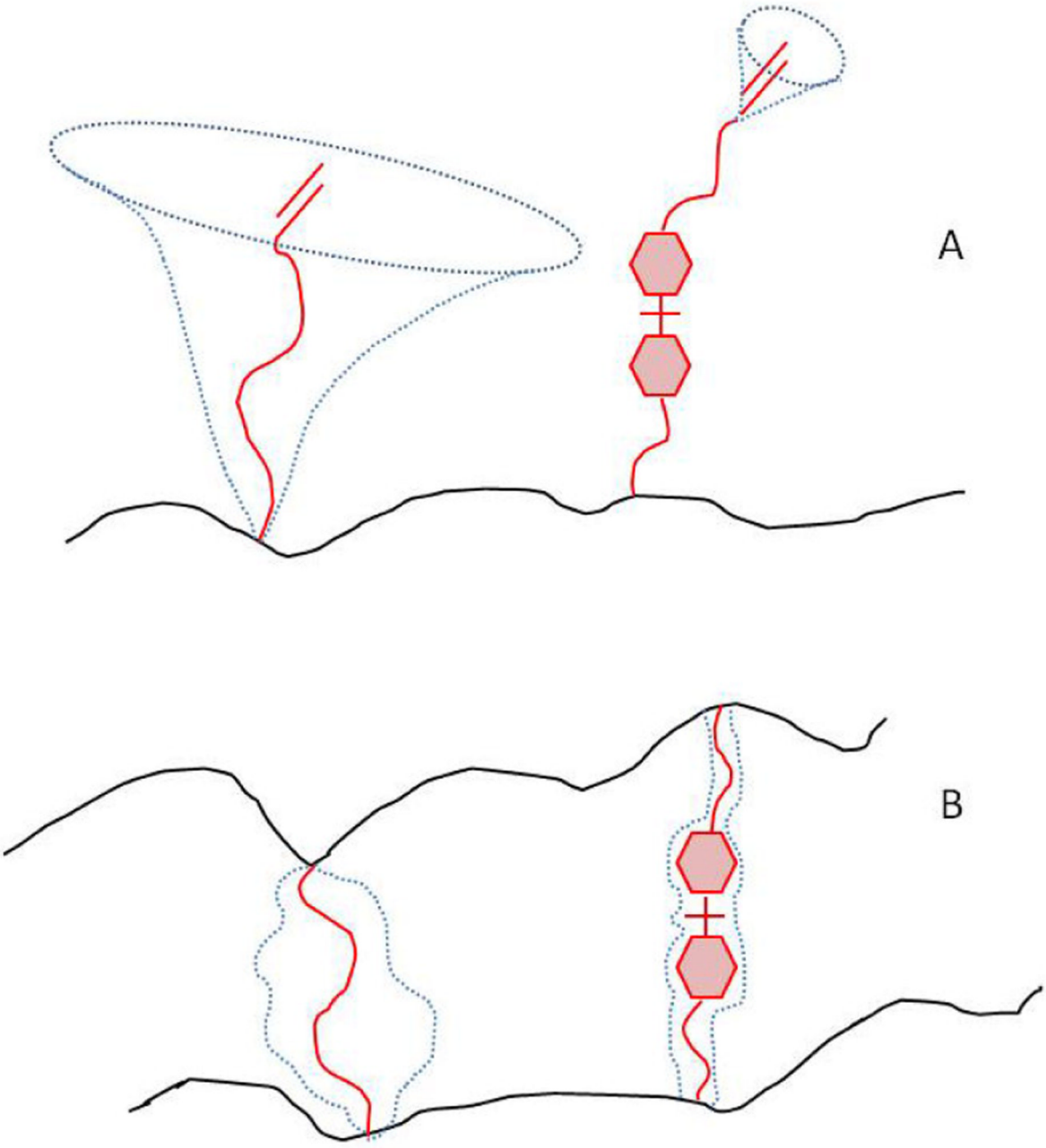

Scheme 1.
Degrees of freedom of (A) pendant groups and (B) crosslinks formed by the aliphatic TEGDMA and the aromatic BisGMA (in red). The dotted lines show the space occupied by each molecule's motion.

Table 1

Kinetic parameters for all different compositions photo-activated for 600 s.

TEGDMA content (mol%)	DC, %	Rp_{max}, $\%/s^{-1}$	DC (%) at Rp_{max}	Rp ($\%/s^{-1}$) at 10% DC	Viscosity, Pa s
100	81.3 (1.7)a	1.0 (0.3)c	37.0 (3.0)a	0.5 (0.1)e	0.015
80	80.8 (3.0)ab	2.6 (0.6)b	33.7 (3.1)ab	1.5 (0.2)d	0.047
60	72.4 (0.3)bc	3.2 (0.1)a	22.7 (1.1)b	2.8 (0.1)b	0.333
40	67.9 (0.8)cd	3.6 (0.1)a	16.8 (1.0)c	3.2 (0.1)a	2.680
20	60.9 (0.2)d	2.4 (0.1)b	12.2 (0.8)c	2.4 (0.0)c	31.670
0	50.2 (2.4)e	0.6 (0.1)c	16.5 (5.7)c	0.4 (0.1)e	-

Table 2

Volumetric shrinkage, pore fraction and extraction results for all different compositions photoactivated for 600 s.

TEGDMA content (mol%)	Pore fraction before extraction (nm^3)	Pore fraction after extraction (nm^3)**	BisGMA content in extract (mol%)*	Mass extracted (%)*	BisGMA content in gel (mol%)*	Volumetric shrinkage (%)
100	2.32 (0.11)a	2.12 (0.20)	0	0.2	0	11.7 (1.0)a
80	2.19 (0.01)ab	2.24 (0.26)	43	0.3	19.9	9.5 (0.6)b
60	2.09 (0.01)ab	2.14 (0.04)	69	0.4	39.9	7.5 (0.4)c
40	2.01 (0.01)b	2.05 (0.04)	76	8.5	58.6	6.0 (0.7)cd
20	1.99 (0.01)b	1.99 (0.19)	93	24.5	76.1	5.4 (0.7)d
0	2.08 (0.01)b	2.02 (0.10)	100	45.8	100	3.5 (0.3)e

*Standard deviations for the percentage values were all below 0.01%.

**All statistically similar (p=0.0313).

Table 3

Final degree of conversion, volumetric shrinkage, pore size and extraction results for BTEG 60-40 composition photoactivated for 10, 20, 30, 60 or 600 s.

Exposure time (s)	DC (%)	Pore size before extraction (nm^3)	Pore size after extraction (nm^3)**	BisGMA content in extract (mol%)*	Mass extracted (%)*	BisGMA content in gel (mol%)*	Volume shrinkage (%)
10	44.5 (0.8)e	2.58 (0.01)a	2.34 (0.13)	54	43.1	64.8	4.4 (0.2)
20	53.1 (0.6)d	2.29 (0.01)b	2.06 (0.07)	59	32.9	60.5	5.0 (0.5)
30	56.5 (0.7)c	2.30 (0.01)b	2.07 (0.01)	59	28.6	60.4	5.8 (0.4)
60	60.5 (1.1)b	2.13 (0.01)c	2.06 (0.11)	62	22.4	59.4	5.7 (0.1)
600	67.9 (0.8)a	2.01 (0.01)d	2.05 (0.04)	76	8.5	58.6	6.0 (0.7)

* Standard deviations for the percentage values were all below 0.01%.

** All statistically similar (p=0.066).

Eur Polym J. Author manuscript; available in PMC 2012 February 1.